Photodetachment and Doppler laser cooling of anionic molecules

Sebastian Gerber, Julian Fesel, Michael Doser, Daniel Comparat

PAPER • OPEN ACCESS

Photodetachment and Doppler laser cooling of anionic molecules

New Journal of Physics
The open access journal at the forefront of physics

Deutsche Physikalische Gesellschaft DPG
IOP Institute of Physics

Published in partnership with: Deutsche Physikalische Gesellschaft and the Institute of Physics

OPEN ACCESS

RECEIVED
10 October 2017

REVISED
22 December 2017

ACCEPTED FOR PUBLICATION
19 January 2018

PUBLISHED
7 February 2018

PAPER

Photodetachment and Doppler laser cooling of anionic molecules

Sebastian Gerber[1,3,4], **Julian Fesel**[1,3], **Michael Doser**[1] and **Daniel Comparat**[2]

[1] CERN, European Laboratory for Particle Physics, 1211 Geneva, Switzerland
[2] Laboratoire Aimé Cotton, CNRS, Université Paris-Sud, ENS Paris Saclay, Université Paris-Saclay, Bât. 505, F-91405 Orsay, France
[3] These authors contributed equally to this work.
[4] Author to whom any correspondence should be addressed.

E-mail: sebastian.gerber@cern.ch

Keywords: non neutral plasma, anionic molecules, sympathetic Doppler cooling, Penning trap

Abstract

We propose to extend laser-cooling techniques, so far only achieved for neutral molecules, to molecular anions. A detailed computational study is performed for C_2^- molecules stored in Penning traps using GPU based Monte Carlo simulations. Two cooling schemes—Doppler laser cooling and photodetachment cooling—are investigated. The sympathetic cooling of antiprotons is studied for the Doppler cooling scheme, where it is shown that cooling of antiprotons to subKelvin temperatures could becomes feasible, with impacts on the field of antimatter physics. The presented cooling schemes also have applications for the generation of cold, negatively charged particle sources and for the sympathetic cooling of other molecular anions.

1. Introduction

Atomic and molecular anions are relevant in a variety of different fields starting from the chemistry of highly correlated systems [1], the studies of planetary atmospheres [2], negative superhalogens [3] to the interstellar medium [4, 5]. The study of the processes in which the anions are involved is currently hampered by their synthesis at ultracold temperatures. Up to now, temperatures of at best several Kelvin have been achieved via supersonic expansion of anionic gas followed by resistive, buffer gas or electron cooling in cryogenic environments [6–11]. The utilization of laser cooling techniques, routinely used for neutrals, positive ions and neutral molecules (SrF, YO, CaF) [12–14], could for the first time allow the investigation of anionic systems at subKelvin temperatures. In a broader perspective, cooling even a single anion species would enable one to cool any other negatively charged particles via sympathetic cooling including e^-, atomic and molecular anions and antiprotons. The latter are relevant for antihydrogen ($\bar{H}$) experiments, since even though first spectroscopic results on the 1S–2S transition of $\bar{H}$ have been recently obtained [15], their current sensitivity to CPT violations is not yet competitive with that obtained with antiprotons [16, 17] or positrons [18]. Further, measuring the gravitational interaction between matter and antimatter with similar precisions as has been accomplished for matter experiments [19, 20] requires full control of the external and internal state of $\bar{H}$ and temperatures below mK. More generally, the precision of future $\bar{H}$ experiments strongly correlates with the temperature at which $\bar{H}$ can be prepared. Current techniques that rely on forming $\bar{H}$ by interacting $\bar{p}$ and e^+ which have been pre-cooled in a cryogenic Penning trap achieve $\bar{H}$ temperatures in the region of 10 K [15]. The creation of ultracold $\bar{H}$ via the resonant charge exchange of antiprotons with ortho-positronium (o-Ps) is potentially, limited only by the recoil limit of the constituents [21].

This goals of obtaining ultracold $\bar{H}$ has recently sparked theoretical and experimental investigations to use laser-cooled atomic anions like Os^- and La^- [10, 22–24]. As another approach to this yet-to-be-realized procedure, molecular anions are a potential candidate for laser cooling down to the mK regime and have been studied in [11]. In [25] a Sisyphus cooling scheme using optical dipole forces was investigated including the sympathetic cooling of other anions. Here, similarly to Doppler cooling, optical dipole force cooling relies on multiple lasers that repump the population of the coolant in a quasi closed cycle.

In this article, an easy-to-implement scheme relying only on two optical transitions is presented as photodetachment cooling. In this scheme, a selective fraction of C_2^- molecules with high kinetic energies can be

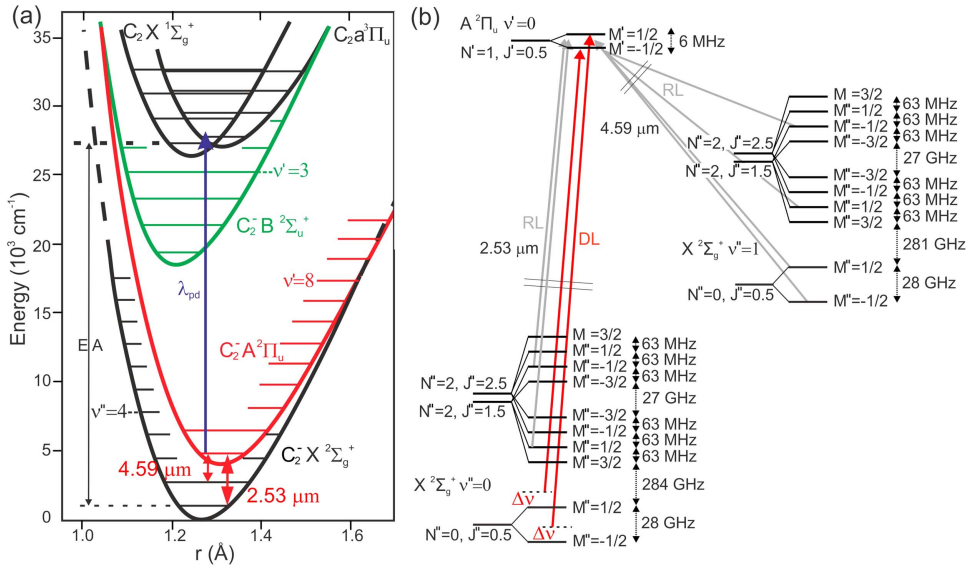

Figure 1. (a) Molecular potential energy of C_2^- versus internuclear separation with the electronic and vibrational levels including two neutral C_2 ($X^1\Sigma_g^+$, $a^3\Pi_u$) curves [37]. The *X*–*A* (red) cooling transitions and the photodetachment (blue, λ_{pd}) transition are indicated with arrows. (b) Zeeman splitted vib–rot sublevels in a 1 T field showing the laser for the Doppler cooling scheme. The electron spin $\frac{1}{2}$ is coupled to the rotational quantum number *N* to form the full angular momentum *J* and its projection *M* on the magnetic field axis. The $v'' = 0$ and $v'' = 1$ manifold of the *X* state and the excited *A* states are shown (not to scale). The two Doppler cooling lasers (DL, red) addressing the ground states at 2.54 μm are depicted with their detunings $\Delta\nu$. The six repumping lasers are sketched (RL, gray) at 2.54 μm and 4.59 μm, respectively. Reproduced from [25]. CC BY 4.0.

removed by two-stage laser induced photodetachment, hereby reducing the temperature of the remaining particles after reaching plasma equilibrium once again. While commonly applied for the spectroscopy of anionic systems [26, 27] and recently for the controlled manipulation of the internal states of molecular anions [28], photodetachment is, to our knowledge, for the first time investigated for the purpose of cooling trapped anions in Penning traps. In [29] evaporative cooling of anions in a rf trap was theoretically investigated using one laser slightly detuned below the photodetachment threshold. Further, in this article the feasibility of the sympathetic cooling of antiprotons in a Penning trap under realistic experimental conditions are discussed using the Doppler cooling method. Both studies are performed on the molecular anion C_2^-. Among many possible candidates, C_2^- has the advantage of a well-known level structure and due to its homonuclear character the $B^2\Sigma_u^+ \rightarrow A^2\Pi_u$ decay channel is forbidden [30–34]. Furthermore, it has well suited branching ratios between $B^2\Sigma(v' = 0) \leftrightarrow X^2\Sigma(v'' = 0)$ ground vibrational states of 72% and between $A^2\Pi_{1/2}(v' = 0) \leftrightarrow X^2\Sigma(v'' = 0)$ of 96%. In comparison to atomic La^-, molecular C_2^- has a similar dipole transition but exhibits no unwanted photodetachment, no hyperfine structure and can be produced at low sub-eV kinetic energies [35]. Figure 1(a) shows an overview of the electronic and vibrational level structure of C_2^- and C_2. The potential curves of the molecule were calculated using the empirical function proposed in [36], using spectroscopic parameters from [32, 37]. The vibrational levels are based on constants from [37]. For C_2 the curves where shifted by the electron affinity EA = 3.269. The rot–vib and electronic spectra of C_2^- were simulated using the program PGOPHER [38].

2. Sympathetic Doppler cooling of $C_2^-/\bar{p}$

C_2^- can be produced from plasma discharge of acetylene with internal energies in the sub-eV range at densities of 10^{13} m^{-3} [35, 39]. After selection of C_2^- in a mass spectrometer, the anions can be trapped in a Penning trap. In sequence, $\bar{p}$ can be trapped in the same Penning trap at a different axial position. Starting from typical experimental conditions that are achieved at CERN's Antiproton Decelerator facility approximately 10^5 $\bar{p}$ can be caught and initially electron-cooled to eV kinetic energies [15, 40–42]. The $\bar{p}$ can then be mixed with the C_2^- and with priorly loaded e^- using potential manipulations, similarly as demonstrated in the preparation of different charge-to-mass-ratio species plasmas [43, 44]. Using electron cooling after the mixing process and considering a 1 T Penning trap at 10 K, temperatures of the $C_2^-/\bar{p}/e^-$ ensemble around 100 K can be realized within a few tens of seconds [45]. Subsequently, by lowering the axial trapping potential confining the particles allows for additional evaporative cooling and the preparation of the mixed plasma at about 10 K [46].

In the trap the $\mathbf{E} \times \mathbf{B}$ field causes an azimuthal drift of the particles about the magnetic field axis. At a same radius the difference in mass of the two species will result in a difference in centrifugal force and with that

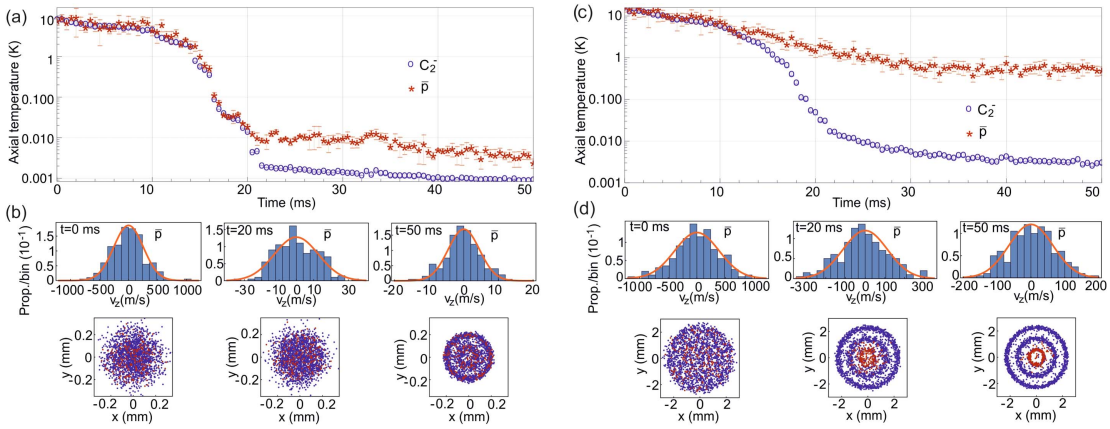

Figure 2. Simulation of sympathetic cooling in a 1 T Penning trap for a Coulomb factor of (a) $C_f = 1$ and (c) $C_f = 5000$ using a Doppler cooling force scaled by 10^4, see text for details. The confidence intervals are obtained from Boltzmannian fits to the particle velocity distributions. The temperature evolution of 1848 C_2^- (solid, red) and 200 $\bar{p}$ (dotted, blue) are calculated. In both plots the laser detunings are adjusted to the half width of the Doppler broadened Voigt profile in 4 steps from $\Delta\nu = -39$ MHz to $\Delta\nu = -3.4$ MHz using a laser linewidth of $\delta\nu = 1$ MHz. Histogram of the axial velocity distribution in (b) for $C_f = 1$ and (d) for $C_f = 5000$ together with the radial plasma profile for three corresponding times for C_2^- (red) and $\bar{p}$ (blue).

rotation rate. Collisional drag gives rise to a separation of the particles with the lighter $\bar{p}$ drifting inwards and the heavier C_2^- outwards. In thermal equilibrium the rotation of the plasma is rigid at a frequency ω_r [43]. In the limit of zero Debye length, the density n_j of species j is then determined by ω_r as $n_j = 2\epsilon_0 m_j \omega_r(\Omega_j - \omega_r)/e^2$, with m_j and Ω_j the respective mass and cyclotron frequency [43]. For the case of $\Omega_j \gg \omega_r$ the plasma will evolve to a spheroidal shape with approximately equal densities and $\omega_r = e\,n/(2\epsilon_0 B)$. Axially, the particles oscillate with a frequency $\omega_{z,j} = 2\pi \times \nu_{T,j}/2l_j$, with $\nu_{T,j} = \sqrt{kT_z/m_j}$ the thermal velocity and trapping length l_j.

In order to study the effect of sympathetic cooling, figure 2(a) shows a simulation of Doppler cooling a $C_2^-/\bar{p}$ plasma confined in a 1 T Penning trap. The Coulomb particle–particle interaction and the trapping field is simulated for a total of 1848 C_2^- and 200 $\bar{p}$ with time steps that resolve the cyclotron motion of the $\bar{p}$ including N-body space charge effects. To scale the simulation to experimentally typical particle numbers of $N_{\bar{p}} \sim 10^5$ with a particle ratio of $N_{C_2^-} \sim 10N_{\bar{p}}$ and to investigate possible geometrical plasma effects the Coulomb interaction force between the particles is increased by a factor $C_f = 5000$ without affecting the particle-trap interaction. For this case, the simulation is shown in figure 2(c). The computation is performed on a GPU running on the mass parallel platform CUDA and the N-body algorithm described in [47]. A fifth order Dormand–Prince integrator is used to calculate the force equation each time step [48].

To implement Doppler cooling in the simulation, the lasers are applied along the z-axis and parallel to the magnetic trapping field, that acts as a quantization axis. In this configuration only $\Delta M = \pm 1$ laser transitions are allowed, whereas spontaneous decays from the excited states can occur on $\Delta M = 0, \pm 1$ transitions. Figure 1(b) depicts the relevant vib–rot C_2^- levels in the 1 T field together with the lasers for Doppler cooling. The transition strength probabilities of the excited $|A,\ v' = 0,\ N' = 1\rangle$ state to the X state vibrational levels are $96, 4, 2 \times 10^{-6}$ (percentage of the Franck–Condon); the natural linewidth of the excited state is $\Gamma_{sp} = 2\pi \times 3.13$ kHz [30, 32–34, 37]. Two narrow-band lasers at 2.53 μm address the two $\left|X,\ v'' = 0,\ N'' = 0,\ M'' = \pm\frac{1}{2}\right\rangle \rightarrow \left|A,\ v' = 0,\ N' = 1,\ M' = \mp\frac{1}{2}\right\rangle$ transition. The cooling lasers are red detuned from resonance by $\Delta\nu$. In order to achieve a quasi closed transition cycle of the populations two additional 2.53 μm lasers repump the $|X,\ v'' = 0,\ N'' = 2,\ J'' = 2.5,\ 1.5\rangle$ manifolds with imprinted sideband structures at 63 MHz (The power ratios of the carrier, first and second order sideband are considered with a modulation index of 1.8 as $I0 \approx 2I1 \approx I2$). Each repump laser then addresses four $\Delta M = \pm 1$ transitions. From each of the two excited A states there are six allowed $\Delta M = 0, \pm 1$ transitions back to X into the $J'' = 1.5, 2.5$ states and two transitions into the $J'' = 0.5$ states. In a similar way, a total of four additional repump lasers at 4.59 μm are required to address the $|X,\ v'' = 1\rangle$ ro–vib levels. In total 20 laser induced transitions and 32 spontaneous decays are to be considered for the quasi closed cycle.

In the limit of $\Gamma_{sp} \ll \delta\nu$, assuming typical IR-DFB laser linewidths of a few MHz in the simulation, the average cooling force from the Doppler cooling transitions [49, 50] is calculated for each time step using Einstein's rate equations [51]. In steady-state the population is then evenly distributed between all molecular substates. Thus, molecules resonant with the detuned Doppler lasers are selected in the force equation and experience a net cooling force $F_i = lA_i\hbar k_i$ per time step, with k_i the wave vector of the respective cooling transition i. Here, A_i is the Einstein coefficient of one of the two Doppler cooling transitions and l is the fraction of the steady-state population in the excited state as $l = 1/\sum_j = 0.045$, as inverse to the number of all levels j from figure 1(b). For the simulation, the

Doppler and repumper lasers are calculated with circular polarizations and linewidths of $\delta\nu = 1$ MHz and linear polarizations and linewidths of $\delta\nu = 3$ MHz, respectively. For all lasers a power of 3 mW and a waist of 1.5 mm is used. The resulting average cooling force leads to a cooling time on the order of several seconds per Kelvin. In order to simulate the plasma evolution over a wide temperature range within practically accessible simulation times the cooling force used in the following simulations is increased by a factor of 10^4.

The particles are initialized at a temperature of ~10 K and at a density of $n = 8 \times 10^{11}$ m^{-3}. For the case of $C_f = 1$ in figure 2(a) cooling of the C_2^- together with sympathetic cooling of $\bar{p}$ is seen to temperatures of ~4 mK after 50 ms. Without the factor 10^4 increase in the cooling force and for the parameters used in figure 2, the average number of scattered photons then corresponds to 1.3×10^5, with the velocity removed per photon recoil from the two cooling transitions as $\Delta v_i = \hbar k_i / m_{C_2^-}$. Due to the unpumped $|X,\ v'' = 2\rangle$ states, after Doppler cooling a total of 26% of the anions are then expected to end up in these excited vibrational states.

For the plots in figure 2, the temperature values are obtained from Boltzmannian fits of the velocity histograms in axial z direction, pictured in figure 2(b) for $\bar{p}$ at three different times together with the corresponding radial plasma profiles in the x–y plane. At C_2^- temperatures of 1.3 mK the coupling parameter that describes the correlated system as $\Gamma = e^2/(4\pi\epsilon_0 akT)$ with the Wigner–Seitz radius $a = (3/4\pi n)^{1/3}$ approaches values of $\Gamma \sim 174$, where the first-order liquid-solid phase transition to a crystalline plasma state is expected. The crystallization process is visible in the formation of radial plasma patterns as a function of the plasma aspect ratios, density and magnetic field [52], which are precursors to the formation of bcc-lattice planes [43]. For the present trapping geometry two shells are exhibited with an outer plasma radius of $R_p = 0.2$ mm. No pronounced centrifugal separation of the two species is visible, with the separation length defined by $l_{sep} = kT/(|m_{C_2^-} - m_{\bar{p}}|\omega_r^2 R_p)$ reaching values of R_p for temperatures of $T \sim 10$ mK [43]. In figure 2(c) using $C_f = 5000$ and leaving all other parameters identical the particles attain temperatures of 3 mK and 500 mK for C_2^- and $\bar{p}$, respectively, after a simulated time of ~50 ms with the onset of a temperature difference at about 3 K. Introducing the Coulomb factor C_f effectively scales the coupling parameter $\Gamma_c = C_f^{2/3}\Gamma$ with $a_c = C_f^{1/3}a$. At 3 K Γ_c yields about 174, where the formation of three radial shells are visible for the present parameters. Here, with $l_{sep} \ll R_p$ centrifugal separation of the two species starts to be visible at a simulated cooling time of 20 ms with the lighter $\bar{p}$ predominantly concentrated in the inner shell limiting the sympathetic cooling via viscous drag to the outer C_2^-. Further, by increasing C_f close binary collisions dominate to produce equipartition of the axial and radial motions, where the equipartition rate becomes exponentially small with increasing b/r_c, the ratio of the distance of the closest approach $b = e^2/(4\pi\epsilon_0 kT_z)$ and the cyclotron radius $r_c = v_{Tj}/\Omega_j$ of the two species [53, 54]. This effect further contributes to the observed difference in final temperature between the C_2^- and $\bar{p}$.

We have further checked an intermediate simulation using $C_f = 100$ where the onset of the temperature difference occurs at about 0.2 K with the final temperatures of 30 mK for $\bar{p}$ and 10 mK for C_2^- consistent with a crystallization and the Γ_c scaling. The simulations shown in figure 2 indicate that for the typical parameters considered, sympathetic cooling of $\bar{p}$ using C_2^- is expected to work over a large range of temperatures down to subKelvin. Further, the sympathetic cooling occurs within about 1 ms in agreement with [55] on time scale much faster than the effect of the amplified Doppler cooling. This still holds for the simulation including a Coulomb factor.

3. Photodetachment cooling of C_2^-

To cool species with multilevel structures such as C_2^- using the Doppler scheme requires mastering a full set of lasers to absolute frequency precisions on the order of MHz. Additionally, for species faced with narrow dipole transitions cooling times of the order of minutes have to be considered against plasma heating rates in Penning traps [56]. As a different cooling method we shall now study photodetachment cooling relying on only two lasers. Here, a Doppler selective laser with energy $E_D = hc/2.53\ \mu$m (1 MHz, 3 mW) and a waist of 1 mm addresses the $\left|X,\ v'' = 0,\ N'' = 0,\ M'' = \frac{1}{2}\right\rangle$ ground state. By that a fraction of molecules in a velocity window resonant with the laser field is transferred to the excited state $\left|A,\ v' = 0,\ N' = 1,\ M' = \frac{1}{2}\right\rangle$; for cooling the laser frequency is chosen to select molecules with high kinetic energy. From the excited A state, a second laser at λ_{pd} then transfers the population above the photodetachment threshold, EA, splitting C_2^- into neutral C_2 and photoelectrons, see figure 1(a).

In order not to address the ground states the energy of the photodetachment laser $E_{pd} = hc/\lambda_{pd}$ must be $E_{pd} < \mathrm{EA}$. The corresponding total photodetachment cross section σ_A from the state $|A,\ v' = 0\rangle$ for varying photon energy E_{pd} can be calculated as the sum over the partial cross sections σ_p for all quantum numbers i of the C_2 states obeying energy conservation, $\sigma_A(E_{pd}) = \sum_i \sigma_p P_{FC}$ [57, 58], where σ_p is derived by Geltman for homonuclear diatomic anions in [59] and P_{FC} is the relative weight of the transition given by the Franck–Condon factor. A calculation including the molecular potential energies shown in figure 1(a) results in a lower limit of $\sigma_A/\mathrm{cm}^2 = 3.5 \times 10^{-17}$ [60, 61]. The cross section for E_{pd} close to the threshold $\mathrm{EA} - E_D$ is significantly lower reaching $\sigma_A/\mathrm{cm}^2 \sim 1 \times 10^{-19}$. The expected photodetachment rate is then given by $\Gamma_{pd} = \sigma_A I/E_{pd}$ for a laser intensity I and has to be seen in comparison to the total natural decay rate of the excited state of $\Gamma_{sp} = 19.7\ \mathrm{ms}^{-1}$ [32, 33]. Experimentally $\Gamma_{pd} > \Gamma_{sp}$ can, for example, be realized with a frequency-doubled Ti:sapphire laser system

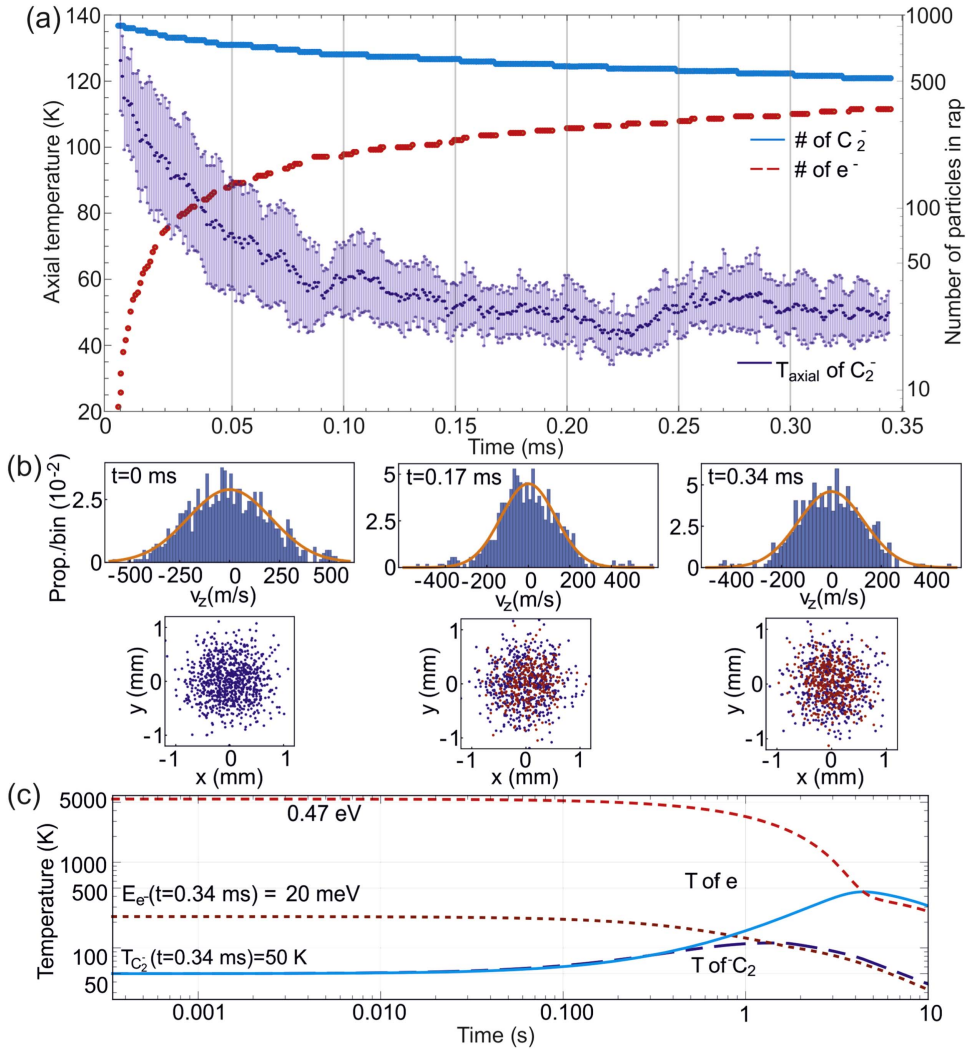

Figure 3. (a) Simulation of photodetachment cooling in a 1 T Penning trap at $C_f = 1$ and $E_{e^-} = 20$ meV, see text for detail. The temperature evolution of initially 1000 C_2^- (blue) is simulated together with the created photoelectrons. The initial laser detuning of the 2.53 μm laser is set to 1σ of the initial Doppler profile width as $\Delta\nu = 116$ MHz and is linearly swept to $\Delta\nu = 84$ MHz. (b) Velocity histograms at three different times with the corresponding radial plasma profile of C_2^- (blue) and e^- (red). (c) Calculation of the C_2^-/e^- temperature evolution caused by photoelectrons with energy $E_{e^-} = 0.46$ eV for C_2^- (solid, blue) and e^- (dashed, red) and $E_{e^-} = 20$ meV for C_2^- (dashed–dotted, dark blue) and e^- (dotted, dark red). $N_{C_2^-}/N_{e^-} = 1.5\ \eta$ and initial $T_{C_2^-} = 50$ K.

enhanced in a low finesse cavity at 380 nm (3.26 eV) close to the *EA* threshold. While the neutral C_2 molecules will escape the trapping potential after photodetachment of C_2^-, the released photoelectrons will continue to Coulomb-interact with the plasma. The photoelectrons' angular distribution hereby depends on the angular momentum of C_2^-. The distribution can be described by the Cooper–Zare model [62, 63] and for simplicity will be approximated by an isotropic character for the following simulation. The kinetic energy of the photoelectrons is dominated by the residual binding energy given by the difference between the combined photon energy and the photodetachment threshold, $E_{e^-} = E_{\mathrm{pd}} + E_D - \mathrm{EA}$, and can take values of $E_{e-} < 0.47$ eV. Only the fraction of released electrons which have a kinetic energy projection along the trap axis smaller than the axial confinement potential of the space charge plasma U will stay trapped. This can be expressed by the limit angle $\beta = \mathrm{acos}\,(\sqrt{U/E_{e^-}})$ that defines the fraction of trapped photoelectrons as $\eta = 1 - \int_0^{\beta} \sin(\phi)\,\mathrm{d}\phi$. These electrons will thus continue to equilibrate with the plasma due to Coulomb collisions and their coupling to the black-body radiation of the environment.

The described processes are simulated in figure 3(a) for 1000 C_2^- particles in a 1 T Penning trap for a photodetachment rate of $\Gamma_{\mathrm{pd}} = 85\ \mathrm{ms}^{-1}$ and an axial confinement of $U = 20$ mV. Employing Einstein's optical rate equations on all relevant transitions shown in figure 2(b), the pumping and photodetachment process is included using the Monte Carlo method. In the simulation, the plasma is first initialized at a density of $n = 5 \times 10^{12}\ \mathrm{m}^{-3}$ and $T = 120$ K, which ranges close to temperatures measured using electrostatic plasma modes [64]. The 2.53 μm laser is blue-detuned from resonance to address only the fraction of anions with a high kinetic energy before interacting with a light field at $\lambda_{\mathrm{pd}} = 442$ nm. At this wavelength $E_{e^-} = 20$ meV and all e^- are trapped, $\eta = 1$. By this, molecules with high kinetic are removed from the trapping fields. After reaching

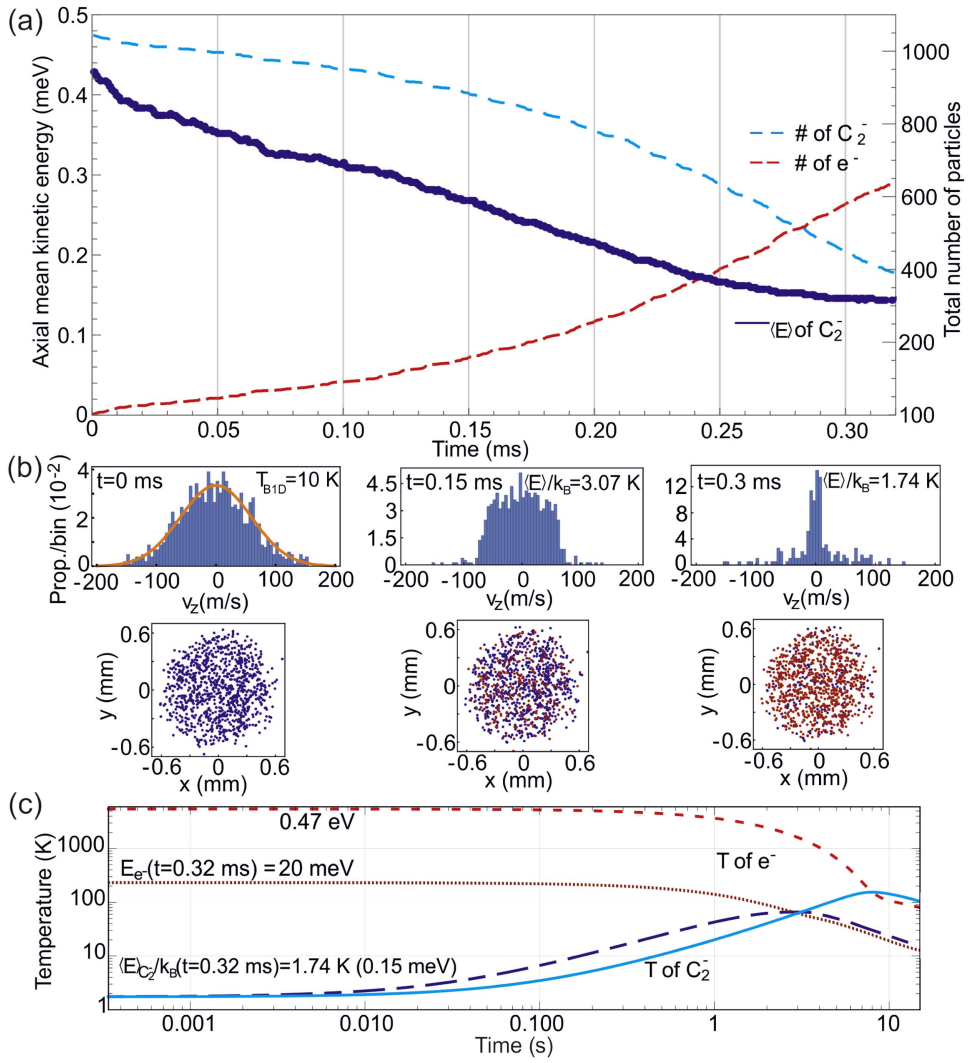

Figure 4. Photodetachment cooling simulation for C_2^- at $C_f = 1$ in a 1 T trap. (a) Evolution of the axial kinetic energy of 1100 molecules after initialization in thermal equilibrium at $T = 10$ K and $E_{e+} = 20$ meV. The detuning of the 2.53 μm laser is linearly swept from initial $\Delta\nu = 60$ MHz to $\Delta\nu = 16$ MHz. (b) Radial plasma profile of C_2^- (blue) and e^- (red) at three different times together with the velocity histograms showing the Boltzmann fit at initialization and two distributions with the corresponding mean kinetic energy in Kelvin. (c) Temperature evolution for the case of photoelectron energies of $E_{e^-} = 0.46$ eV for C_2^- (solid, blue) and e^- (dashed, red) and for $E_{e^-} = 20$ meV for C_2^- (dashed–dotted, dark blue) and e^- (dotted, dark red). $N_{C_2^-}/N_{e^-} = 0.7$ η, for $\langle E\rangle_{C_2^-}/k_B = 1.74$ K.

equilibrium once again [65], the remaining C_2^-/e^- plasma are left with a mean reduced temperature. This process is very similar to evaporative cooling as performed with neutral atoms [66]. The number of C_2^- in the trap decreases until it reaches a saturation level after ~0.35 ms, which is determined by loss of C_2^- in unpumped molecular states. The confidence intervals are obtained from Boltzmannian fits to the particle velocity distribution shown in figure 3(b) together with the radial plasma profiles. The temperature evolution for longer time scales >0.35 ms caused by the released photoelectrons is shown in figure 3(c) for $\lambda_{pd} = 442$ nm and for the case of 380 nm ($E_{e^-} = 0.47$ eV, $\eta = 0.21$). Here a coupled rate equation calculation of the C_2^-/e^- plasma is performed including synchrotron radiation [45] in the trapping field. The final parameters of the GPU simulation from figure 3(a) at $t = 0.34$ ms are used as input values for figure 3(c) as the particle number ratio and the initial temperature of C_2^- and e^-. Here, the temperature of the C_2^- initially follows similar behavior for different photodetachment conditions. After approximately 2–5 s the system reaches temperatures of 100–400 K for increasing e^- energies before electron cooling dominates. From these two plots one infers that for the considered density, B field and initial C_2^- temperature the photoelectron heating occurs on a time scale about 30 times longer than the photodetachment cooling. Thus, in the overall temperature dynamics a temperature minimum is seen after ~0.35 ms at 50 K and is found to be robust for different E_{e-}. It is thus this difference of time scales of the competing processes which allows for the technique of photodetachment cooling. Measurements at cold temperature can be then performed in an experimental window of ~100 ms.

In figure 4 photodetachment cooling is studied for C_2^- at 10 K after electron cooling to the liquid helium Penning trap environment [67]. At this temperature the cooling is initialized with identical trap and laser

parameters as in figure 3. The result of the Monte Carlo simulation using 1100 C_2^- molecules is depicted in figure 4(a). The mean kinetic energy of all anions is calculated from the square of the mean velocities from the histograms shown in figure 4(b). A temperature reduction of a factor of ~5.5 is seen for a C_2^- number decrease by a factor of 2.5 after ~0.32 ms. Figure 4(c) plots the thermalization of C_2^- and photoelectrons for a longer time scale >0.32 ms using rate equations [45] for two different E_{e-}. A window of approximately 10 ms can be used to perform measurements on cold anions which is sufficient for spectroscopic analysis of C_2^- of any sympathetically cooled negative species or pulsed antihydrogen formation [21].

4. Summary

A detailed computational study including all influencing trapping and optical parameters was performed using GPU aided simulations for laser cooling of C_2^- anions and the sympathetic cooling of $\bar{p}$ stored in Penning traps. Photodetachment cooling is discussed for the first time as an accessible method to generate anions in the subKelvin regime. For the typical density and temperature range investigated, this scheme relies on a system of only two commercially available lasers and allows for an approximately 10 ms long time window at ultracold temperatures for experimental measurements. The time window is found to be robust for a wide range of photodetachment energies. Further it was shown, by investigating Doppler cooling, that C_2^- could be a suitable sympathetic coolant for $\bar{p}$ in cryogenic environments enabling their preparation at lower temperatures than currently achieved. Additionally, starting photodetachment cooling at even lower energies, e.g. after Doppler cooling or using a trap at dilution refrigerator temperatures could potentially assist in the preparation of an ensemble of mK $\bar{p}$. This step would permit the resonant charge exchange formation of ultracold antihydrogen [21] (by employing available pulsed positronium sources [68]) and thus allows sensitive studies of CPT symmetries and of the WEP with neutral antimatter systems.

Acknowledgments

We like to thank Viatcheslav Kokoouline for performing the cross section calculations for C_2^-. The research leading to these results has received funding from the European Research Council under Grant Agreement No. 277762 COLDNANO.

ORCID iDs

Sebastian Gerber https://orcid.org/0000-0001-5101-1250

References

[1] Jin D S and Ye J 2012 *Chem. Rev.* **112** 4801–2
[2] Biemann K 2006 *Nature* **444** E6
[3] Freza S and Skurski P 2010 *Chem. Phys. Lett.* **487** 19–23
[4] Li X and Paldus J 2006 *Chem. Phys. Lett.* **431** 179–84
[5] Simons J 2008 *J. Phys. Chem.* A **112** 6401–511
[6] Gerlich D 1995 *Phys. Scr.* **T95** 256
[7] Deiglmayr J, Goritz A, Best T, Weidemuller M and Wester R 2012 *Phys. Rev.* A **86** 043438
[8] Kumar S S, Hauser D, Jindra R, Best T, Geppert W D, Millar T J and Wester R 2013 *Astrophys. J.* **776** 25
[9] Gabrielse G, Khabbaz A, Hall D S, Heimann C, Kalinowsky H and Jhe W 1999 *Phys. Rev. Lett.* **82** 3198
[10] Jordan E, Cerchiari G, Fritzsche S and Kellerbauer A 2015 *Phys. Rev. Lett.* **115** 113001
[11] Yzombard P, Hamamda M, Gerber S, Doser M and Comparat D 2015 *Phys. Rev. Lett.* **114** 213001
[12] Shuman E S, Barry J F and Demille D 2010 *Nature* **467** 820–3
[13] Hummon M T, Yeo M, Stuhl B K, Collopy A L, Xia Y and Ye J 2013 *Phys. Rev. Lett.* **110** 1–5
[14] Zhelyazkova V, Cournol A, Wall T E, Matsushima A, Hudson J J, Hinds E A, Tarbutt M R and Sauer B E 2014 *Phys. Rev.* A **89** 2–6
[15] Ahmadi M 2017 *Nature* **541** 506–10
[16] Ulmer S *et al* 2015 *Nature* **524** 196–9
[17] DiSciacca J *et al* 2013 *Phys. Rev. Lett.* **110** 130801
[18] Dehmelt H, Mittleman R, Van Dyck R S and Schwinberg P 1999 *Phys. Rev. Lett.* **83** 4694–6
[19] Peters A, Chung K and Chu S 1999 *Nature* **400** 849–52
[20] Müller H, Peters A and Chu S 2010 *Nature* **463** 926–9
[21] Doser M *et al* 2012 *Class. Quantum Grav.* **29** 184009
[22] Kellerbauer A and Walz J 2006 *New J. Phys.* **8** 45
[23] Warring U, Amoretti M, Canali C, Fischer A, Heyne R, Meier J O, Morhard C and Kellerbauer A 2009 *Phys. Rev. Lett.* **102** 043001
[24] Pan L and Beck D R 2010 *Phys. Rev.* A **82** 014501
[25] Fesel J, Gerber S, Doser M and Comparat D 2017 *Phys. Rev.* A **96** 031401
[26] Trippel S, Mikosch J, Berhane R, Otto R, Weidemüller M and Wester R 2006 *Phys. Rev. Lett.* **97** 193003
[27] Kim J, Weichman M, Sjolander T, Neumark D, Klos J, Alexander M and Manolopoulos D 2015 *Science* **349** 510

[28] Hauser D et al 2015 Nat. Phys. 11 467
[29] Crubellier A 1990 J. Phys. B: At. Mol. Opt. Phys. 23 3585–607
[30] Rosmus P and Werner H J 1984 J. Chem. Phys. 80 5085
[31] Mead R D, Hefter U, Schulz P A and Lineberger W C 1985 J. Chem. Phys. 82 1723
[32] Špirko T and Šedivcová V 2006 Mol. Phys. 104 1999
[33] Jones P L, Mead R D, Kohler B E, Rosner S D, Lineberger W C, Jones P, Mead R D, Kohler B E, Rosner S D and Unebergerll W C 1980 J. Chem. Phys. 73 4419
[34] Shan-Shan Y, Xiao-Hua Y, Ben-Xia L, Kakule K, Sheng-Hai W, Ying-Chun G, Yu-Yan L and Yang-Qin C 2003 Chin. Phys. 12 745
[35] Tulej M, Knopp G, Gerber T and Radi P P 2010 J. Raman Spectrosc. 41 853–8
[36] Zavitsas A A 1991 J. Am. Chem. Soc. 113 4755–67
[37] Ervin M K and Lineberger W C 1991 J. Phys. Chem. 95 1167–77
[38] Western C M 2017 J. Quant. Spectrosc. Radiat. Transfer 186 221–42
[39] Rehfuss B D, Liu D J, Dinelli B M, Jagod M F, Ho W C and Oka T 1988 J. Chem. Phys. 89 129–37
[40] Gabrielse G et al 2008 Phys. Rev. Lett. 100 113001
[41] Amsler C and Ariga A 2016 J. Phys.: Conf. Ser. 755 011001
[42] Enomoto Y et al 2010 Phys. Rev. Lett. 105 1–4
[43] Dubin D H E and O'Neil T M 1999 Rev. Mod. Phys. 71 87
[44] Jelenković B, Newbury A, Bollinger J, Itano W and Mitchell T 2003 Phys. Rev. A 67 63406
[45] Rolston S L and Gabrielse G 1989 Hyperfine Interact. 44 233–45
[46] Andresen G B et al 2010 Phys. Rev. Lett. 105 1–5
[47] Nyland L, Harris M and Prins J F 2007 GPU Gems 3 677–96
[48] Gorp S V and Dupre P 2013 AIP Conf. Proc. 1521 300
[49] Wineland D J and Itano W M 1979 Phys. Rev. A 20 1521
[50] Eschner J, Schmidt-Kaler F and Blatt R 2003 J. Opt. Soc. Am. B 20 1003
[51] Höppner R, Roldán E, Valcárcel G J D and Optica D 2012 Am. J. Phys. 80 882
[52] Totsuji H, Tsuruta K, Totsuji C, Nakano K, Kamon K and Kishimoto T 1999 AIP Conf. Proc. 498 77–82
[53] Jensen M J, Hasegawa T, Bollinger J J and Dubin D H E 2005 Phys. Rev. Lett. 94 025001
[54] Dubin D H E 2005 Phys. Rev. Lett. 94 025002
[55] Anderegg F, Driscoll C F and Dubin D H E 2010 Phys. Plasmas 17 55702
[56] Andresen G et al 2007 Phys. Rev. Lett. 98 023402
[57] Blumberg W A M, Itano W M and Larson D J 1979 Phys. Rev. A 19 139–48
[58] Barrick J B and Yukich J N 2016 Phys. Rev. A 93 023431
[59] Geltman S 1958 Phys. Rev. 112 176–8
[60] Douguet N, Kokoouline V and Greene C H 2008 Phys. Rev. A 77 064703
[61] Kokoouline V 2016 private communication
[62] Sanov A 2014 Annu. Rev. Phys. Chem. 65 341–63
[63] Surber E, Mabbs R and Sanov A 2003 J. Phys. Chem. A 107 8215–24
[64] Amoretti M et al 2003 Phys. Plasmas 10 3056–64
[65] Anderegg F, Dubin D H E, ONeil T M and Driscoll C F 2009 Phys. Rev. Lett. 102 185001
[66] Petrich W, Anderson M H, Ensher J R and Cornell E A 1995 Phys. Rev. Lett. 74 3352
[67] Amole C et al 2012 Nature 483 439–43
[68] Mariazzi S, Bettotti P and Brusa R S 2010 Phys. Rev. Lett. 104 243401